

# Finite Element Modeling of Electromagnetic Scattering for Microwave Breast Cancer Detection

Reza Firoozabadi<sup>\*1</sup>, Eric L. Miller<sup>2</sup>

<sup>1</sup>Airvana Network Solutions, <sup>2</sup>Tufts University

\*Corresponding author: 19 Alpha Rd., Chelmsford, MA 01824, rfiroozabadi@airvana.com

**Abstract:** Microwave tomography is an imaging modality which uses the contrast between the tissues. The high contrast between breast normal tissue and the malignant tissue makes the microwave imaging a proper option for breast cancer detection. In a typical microwave imaging problem, the breast is illuminated by the microwave antennas surrounding it. Forward model solves the underlying Helmholtz equation to achieve the electromagnetic fields at the location of receiving antennas. The predicted fields may be used in an iterative inversion algorithm to reconstruct the tumor and the other unknown boundaries.

In this paper, we use COMSOL Multiphysics as the finite element forward solver to obtain the electromagnetic fields at the receiving antennas while the breast is illuminated by one antenna in the array. Geometry consists of coronal slices of the breast. The FEM results are then compared with the outcome of an FDFD solver. Numerical results are presented at the end.

**Keywords:** microwave imaging, breast cancer detection, forward models, dielectric properties

## 1. Introduction

In the microwave imaging techniques, breast is illuminated by any of the antennas surrounding it in an array. Resulting scattered waves are measured and can be used to identify the tumor and other unknown boundaries by using an iterative inversion method where the forward model obtains the predicted electromagnetic fields at the location of receiving antennas at each step.

The geometry of our problem consists of breast coronal slices. Each slice is composed of several layers including skin, adipose, and fibroglandular as shown in Figure 1. The tumor is assumed to be located in the fibroglandular layer. A circular array of 16 transceiver antennas embraces the breast. The whole geometry is submerged in a coupling liquid. One antenna radiates and the other non-adjacent antennas acquire the field data.

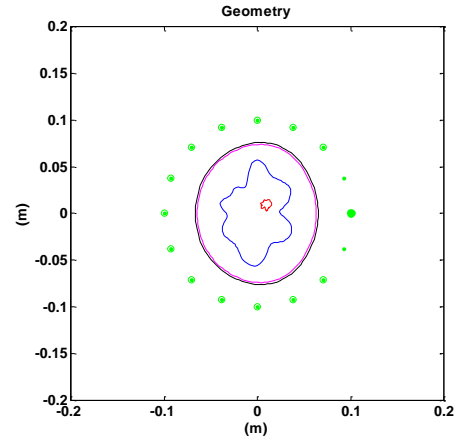


**Figure 1.** Breast cross-sectional geometry consisting of the tumor, fibroglandular, adipose and skin layers (from the innermost to the outermost). One antenna is radiating (shown in bold) and the other non-adjacent antennas are receiving (encircled antennas).

Electromagnetic field components satisfy Maxwell's equations and radiation condition in each breast layer characterized by its complex dielectric properties. The fields scattered by the breast are functions of the geometry and dispersive dielectric properties of the breast tissues.

## 2. Governing Equations

With the antennas located along the  $z$  direction, a TE wave is propagated in the  $x$ - $y$  plane and the governing electric Helmholtz equation in source-free space is [1]:

$$(\nabla^2 + k^2)E_z = 0 \quad (1)$$

where:

$$k^2 = k_0^2 \left( \epsilon_r + i \frac{\sigma}{\omega \epsilon_0} \right) \quad (2)$$

$$k_0 = \omega \sqrt{\mu_0 \epsilon_0} \quad (3)$$

In the above equations,  $\nabla^2$  is the 2-D Laplacian operator,  $k$  is the medium wave number,  $E_z$  is the electric field in  $z$  direction,  $k_0$  is the free-

space wave number,  $\epsilon_r$  is the relative permittivity of the medium,  $\sigma$  is the medium conductivity,  $\omega$  is the angular frequency,  $\epsilon_0$  is the free space permittivity, and  $\mu_0$  is the free space permeability.

Non-zero magnetic field components are derived from  $E_z$  by using Faraday's law in frequency domain as follows:

$$\nabla \times \mathbf{E} = i\omega\mu_0\mathbf{H} \quad (4)$$

or:

$$H_x = -i \frac{1}{\omega\mu_0} \frac{dE_z}{dy} \quad (5)$$

$$H_y = i \frac{1}{\omega\mu_0} \frac{dE_z}{dx} \quad (6)$$

### 3. Dielectric Properties

In a multiple-frequency inversion problem, dispersive dielectric properties of breast tissues are required to be identified versus frequency. Debye formulation of the first or second order has been widely used to model the dispersive media [2]. This model fits the equation coefficients to the measured data and determines the relation between the electric displacement ( $\mathbf{D}$ ) and electric field ( $\mathbf{E}$ ). First-order Debye model is of the form:

$$\epsilon_{rc}(\omega) = \epsilon_r(\omega) + i \frac{\sigma(\omega)}{\omega\epsilon_0} = \epsilon_\infty + \frac{\epsilon_s - \epsilon_\infty}{1 - i\omega\tau} + i \frac{\sigma_s}{\omega\epsilon_0} \quad (7)$$

where  $\epsilon_{rc}$  is the relative complex permittivity,  $\omega$  is the angular frequency,  $\epsilon_r$  is the relative permittivity,  $\sigma$  is the conductivity,  $\epsilon_0$  is the free-space permittivity,  $\epsilon_\infty$  is the relative permittivity at infinite frequency,  $\epsilon_s$  is the static relative permittivity,  $\tau$  is the relaxation time constant, and  $\sigma_s$  is the static conductivity. Hence, the relative permittivity and conductivity are formulated as follows, respectively:

$$\epsilon_r(\omega) = \epsilon_\infty + \frac{\epsilon_s}{1 + (\omega\tau)^2} \quad (8)$$

$$\sigma(\omega) = \omega^2 \tau \epsilon_0 \frac{\epsilon_s - \epsilon_\infty}{1 + (\omega\tau)^2} + \sigma_s \quad (9)$$

Typical parameters for first-order Debye formulation of the breast layers and the tumor are extracted from [3] and [4] and displayed in Table 1. Figure 2 illustrates the values for dielectric properties of breast tissues versus

frequency in skin, adipose, fibroglandular and tumor using first-order Debye model with the typical parameters in Table 1.

**Table 1.** First-order Debye parameters ( $\tau = 15$  ps)

	$\epsilon_\infty$	$\epsilon_s$	$\sigma_s$
Skin	15.3	40.1	0.74
Adipose	3.18	5.02	0.043
Fibroglandular	16.8	36.7	0.461
Tumor	18.8	46.8	0.803

### 4. COMSOL Multiphysics FEM Solver

The geometry of breast layers shown in Figure 1 is implemented by MATLAB and exported to COMSOL Multiphysics. Relative permittivity and conductivity functions in Equations (8) and (9) are defined in COMSOL as analytic expressions. The first-order Debye parameters for the dispersive regions are defined in COMSOL based on the values in Table 1. The matching liquid is taken to be glycerin solution with  $\epsilon_r = 47$  and  $\sigma = 1.36$  at 900 MHz. Spatial distributions of dielectric properties in the breast cross-section are shown in Figure 3 at 900 MHz.

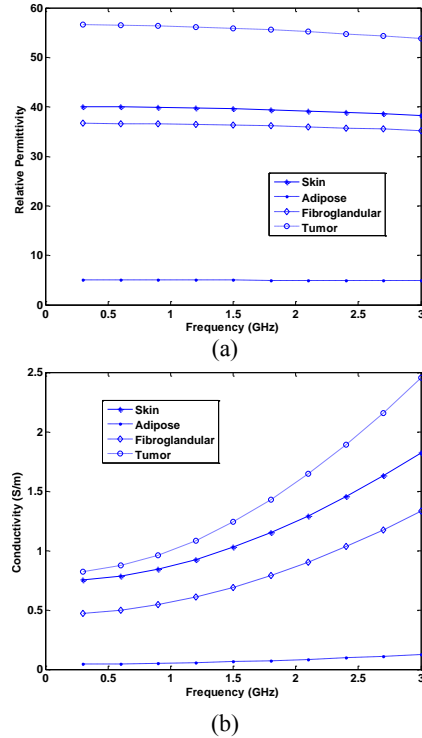


**Figure 2.** Dielectric properties of breast tissues versus frequency: (a) relative permittivity (b) conductivity.

A PML layer of 25 mm width is added around the main geometry in order to terminate our open boundary electromagnetic scattering problem.

COMSOL Multiphysics finite element analysis is performed in RF Module, using In-Plane TE Waves (rfwe) Harmonic propagation analysis type. Adaptive mesh refinement is selected for the solver. The generated mesh is displayed in Figure 4 for the radiating antenna shown in Figure 1.

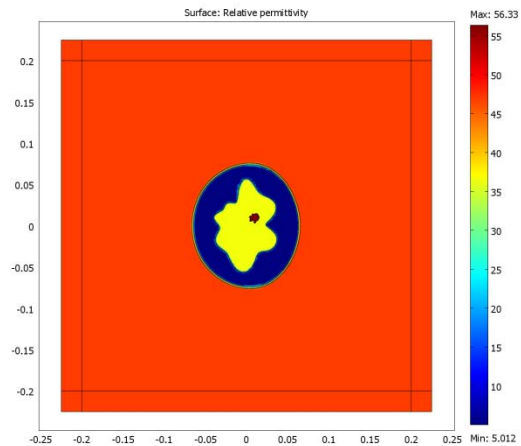
### 5. FDFD Solver

Our FDFD forward solver uses rectangular finite difference discretization of the Helmholtz equation and simulates the propagation of electromagnetic waves in the breast cross-section plane. The FDFD code is written in MATLAB. The same geometry and dielectric properties used in FEM solver are applied to FDFD solver. In order to solve the open-region problem, we use an eight grid cell perfect matched layer (PML) absorbing boundary condition [5]. The grid is taken to be  $601 \times 601$  with the grid spacing equal to  $2/3$  mm.

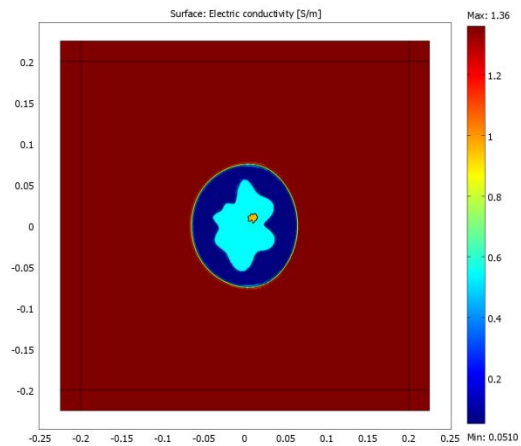
### 6. Experimental Results

The forward problem with the geometry shown in Figure 1 and the dielectric properties explained in previous subsections is solved by both solvers: FEM using COMSOL Multiphysics and FDFD using MATLAB code. One antenna radiates at 900 MHz, while the other 13 non-adjacent antennas collect the electromagnetic fields.

Figures 5, 6 and 7 illustrate the spatial distributions of non-zero electromagnetic fields: electric field  $z$ -component, magnetic field  $x$ -component, and magnetic field  $y$ -component in the whole breast cross-section, respectively. FEM results are compared to FDFD results where magnitude, real part and imaginary part of both simulation types are plotted. The values are truncated for better illustration. Figures 8, 9 and 10 display the non-zero electromagnetic fields: electric field  $z$ -component, magnetic field  $x$ -component, and magnetic field  $y$ -component at the location of receiving antennas, respectively. The results show very good agreement between two forward models.



(a)



(b)

**Figure 3.** Spatial distributions of dielectric properties at 900 MHz plotted in COMSOL Multiphysics: (a) relative permittivity distribution. (b) conductivity distribution (S/m).

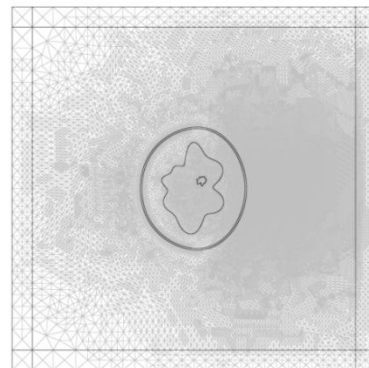


**Figure 4.** Mesh generated by COMSOL Multiphysics using adaptive mesh refinement with the radiating antenna is shown in Figure 1.

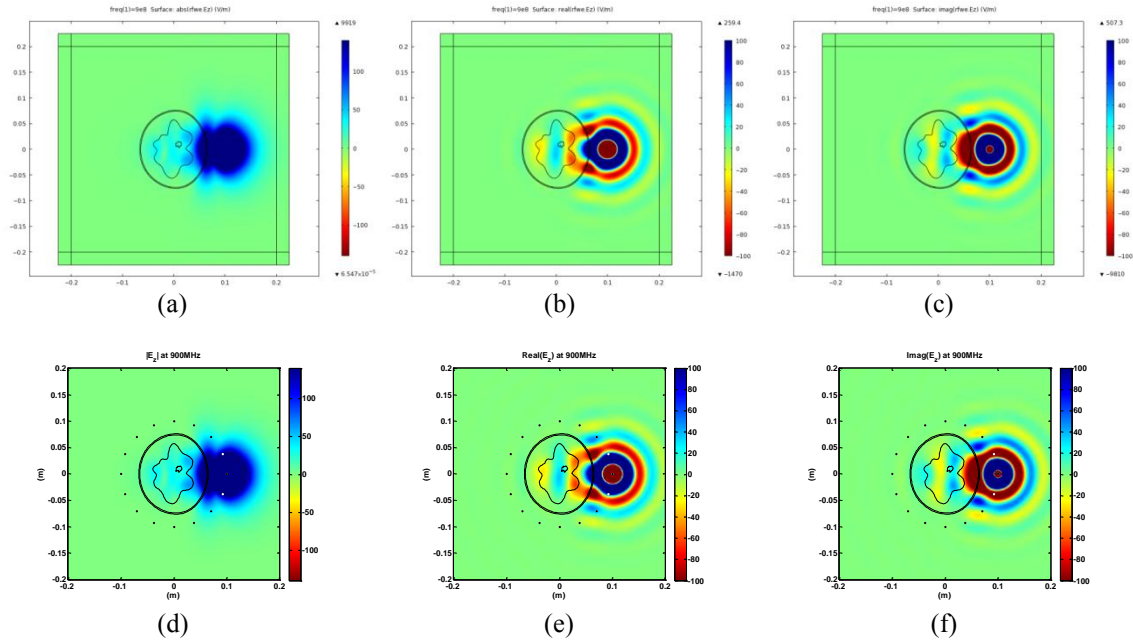


**Figure 5.** Spatial distributions of electric field  $z$ -component ( $E_z$ ) in the breast slice when one antenna is radiating at 900 MHz. FEM results: (a) magnitude (b) real part (c) imaginary part. FDFD results: (d) magnitude (e) real part (f) imaginary part. Values are truncated for better illustration.

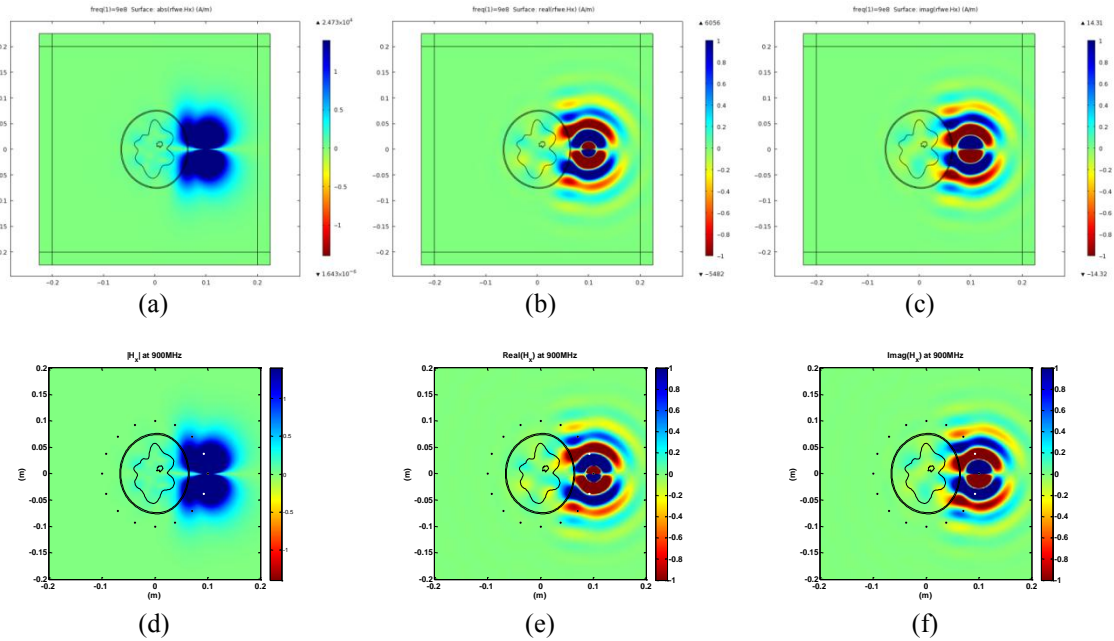


**Figure 6.** Spatial distributions of magnetic field  $x$ -component ( $H_x$ ) in the breast slice when one antenna is radiating at 900 MHz. FEM results: (a) magnitude (b) real part (c) imaginary part. FDFD results: (d) magnitude (e) real part (f) imaginary part. Values are truncated for better illustration.

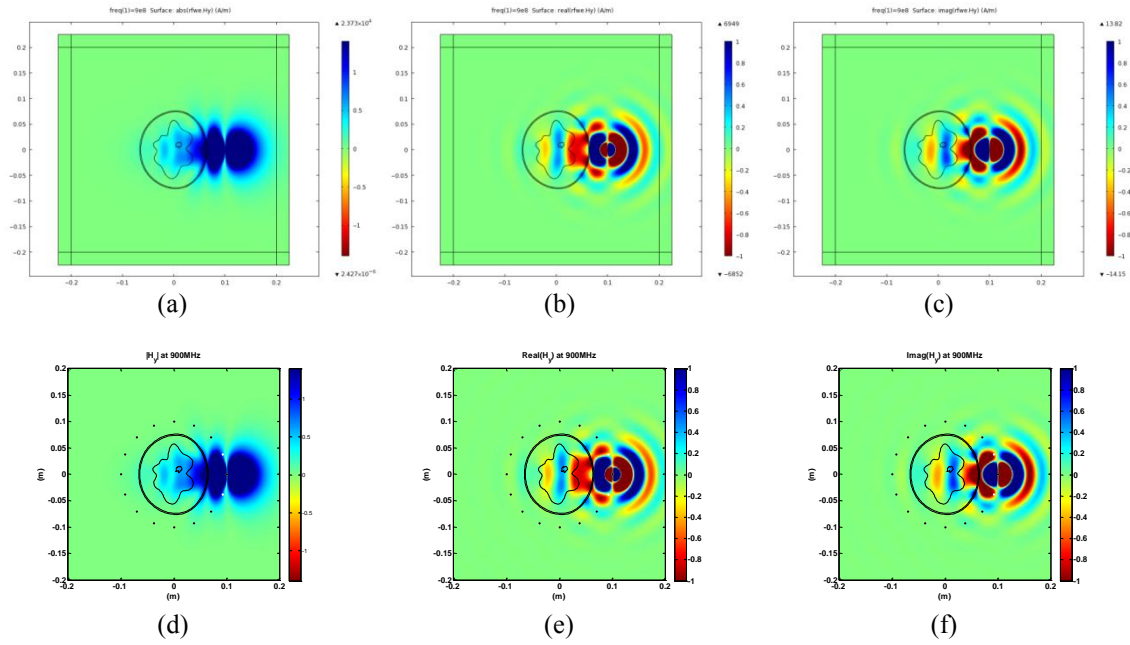


**Figure 7.** Spatial distributions of magnetic field y-component ( $H_y$ ) in the breast slice when one antenna is radiating at 900 MHz. FEM results: (a) magnitude (b) real part (c) imaginary part. FDFD results: (d) magnitude (e) real part (f) imaginary part. Values are truncated for better illustration.

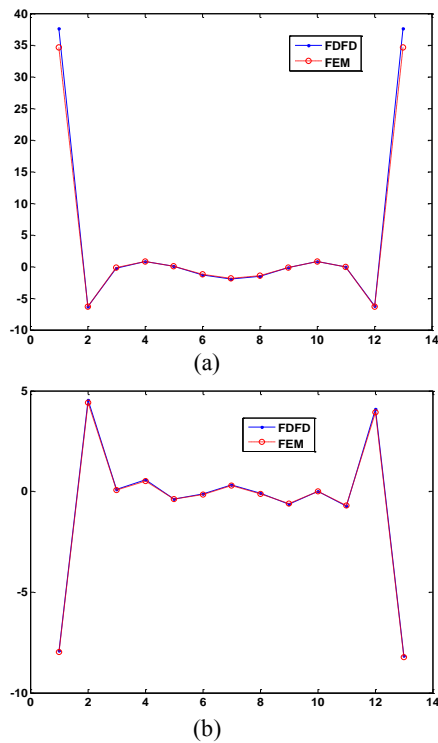


**Figure 8.** Electric field z-component at the location of receiving antennas calculated by FDFD and FEM methods: (a) real part, (b) imaginary part.

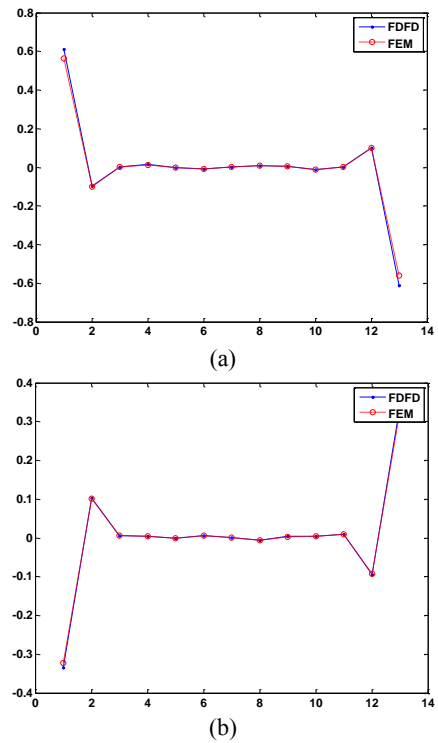


**Figure 9.** Magnetic field x-component at the location of receiving antennas calculated by FDFD and FEM methods: (a) real part, (b) imaginary part.

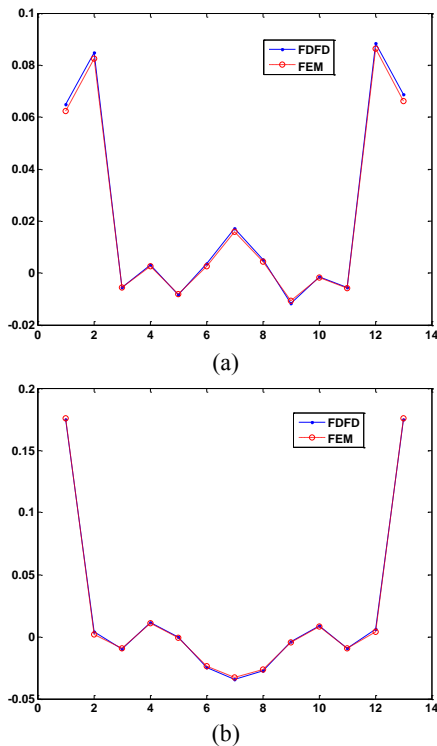


**Figure 10.** Magnetic field  $y$ -component at the location of receiving antennas calculated by FDFD and FEM methods: (a) real part, (b) imaginary part.

## 7. Conclusions

Microwave breast imaging methods use forward models to predict the electromagnetic fields at the location of receiving antennas in order to estimate the unknown geometry parameters by comparing them with observed data. In this paper, we studied the generation of data using FEM by COMSOL Multiphysics software and compared the results with the data generated by our FDFD code written in MATLAB. The results indicate the consistency between two methods. In an iterative procedure, the predicted data calculated at each step can be used to solve the underlying nonlinear optimization problem.

## 8. References

1. D. H. Staelin, A. W. Morgenthaler, and J. A. Kong, *Electromagnetic waves* Englewood Cliffs, NJ:Prentice-Hall, pp. 157-160, 1994.
2. O. Ghandi, "A frequency-dependent finite difference time domain formulation for general

*dispersive media*," IEEE Trans. Microwave Theory Tech., vol. 41, pp. 658-665, 1993.

3. R. W. Lau, S. Gabriel, and C. Gabriel, "The dielectric properties of biological tissues: II. Measurements in the frequency range 10 Hz to 20 GHz," Phys. Med. Biol., vol. 41, pp. 2251-2269, 1996.

4. M. Lazebnik, "A large-scale study of the ultrawideband microwave dielectric properties of normal breast tissue obtained from reduction surgeries," Phys. Med. Biol., vol. 52, pp. 2637-2656, 2007.

5. E. Marengo, C. M. Rappaport, and E. L. Miller, "Optimum PML ABC Conductivity Profile in FDFD," IEEE Transactions on Magnetics, vol. 35, pp. 1506-1509, 1999.